

Self-powered Dynamic Systems in the framework of Optimal Uncertainty Quantification

Farbod Khoshnoud[1]
Department of Mechanical, Aerospace and Civil Engineering,
Brunel University London, Uxbridge, UB8 3PH, United Kingdom
&
Department of Mechanical Engineering, Lyles College of Engineering,
California State University
2320 E. San Ramon Ave., Fresno, CA 93740-8030
kfarbod@csufresno.edu
ASME Member

Ibrahim I. Esat
Department of Mechanical, Aerospace and Civil Engineering,
Brunel University London, Uxbridge, UB8 3PH, United Kingdom
Ibrahim.Esat@brunel.ac.uk

Clarence W. de Silva
Department of Mechanical Engineering,
The University of British Columbia, Vancouver, BC
Canada V6T 1Z4
desilva@mech.ubc.ca
Fellow, ASME

Michael M. McKerns
Divisions of Applied & Computational Mathematics,
California Institute of Technology,
1200 E. California Blvd.
Pasadena, CA 91125, USA
mmckerns@caltech.edu

Houman Owhadi
Divisions of Applied & Computational Mathematics and Control & Dynamical Systems,
California Institute of Technology,
1200 E. California Blvd.
Pasadena, CA 91125, USA
owhadi@caltech.edu

[1] kfarbod@csufresno.edu; farbodkhf@yahoo.com;

ABSTRACT

The energy that is needed for operating a self-powered device is provided by the energy excess in the system in the form of kinetic energy, renewable energy, or a combination of both. This paper addresses the energy exchange issues pertaining to regenerative and renewable energy in the development of a self-powered dynamic system. A rigorous framework that explores the supply and demand of energy for self-powered systems is developed, which considers uncertainties and optimal bounds, in the context of optimal uncertainty quantification. Examples of regenerative and solar-powered systems are given, and the analysis of self-powered feedback control for developing a fully self-powered dynamic system is discussed.

Keywords**:** Self-powered systems, self-powered sensors/actuators, regenerative, solar-powered systems, uncertainty quantification.

Introduction

A self-powered dynamic system [1]-[6] contains fully or partially self-powered devices, which require reduced or no external energy input. The self-powered devices use the excessive, unwanted, or renewable energy in the system, including kinetic energy and other forms of self-generated energy. The energy may be utilized by the self-powered device as it is generated in the system or captured and accumulated (e.g., in a rechargeable battery) for subsequent use as needed. Applications of such self-powered systems are typically associated with sensors and actuators for dynamic systems [1]-[8]. In a self-powered sensor or actuator, harvested or regenerated energy (e.g., vibration kinetic energy or renewable energy) is utilized to provide the required power for the operation of the sensor or actuator. In such a scenario, for example, mechanical kinetic energy/power is converted into electrical energy/power using piezoelectric, electromagnetic or electrostatic mechanisms. Sensors that require low levels of power can harvest the available/excess kinetic energy from the environment and use that energy as a power source [9]-[15]. There are various techniques for optimized harvesting of vibration kinetic energy in self-powered systems. They include frequency tuning using stiffness tuning mechanisms [16], introducing nonlinear dynamics for harvesting energy over a wider frequency range of oscillation [17], and technologies of maximum power point tracking [18]. Electric motors/generators can be used as regenerative actuators for converting kinetic energy into electrical energy [19]-[20]. When used as self-powered devices for vibration control, they can control the same vibration that is induced by the source of kinetic energy (e.g. [21]-[23]). As an example, the power that can potentially be generated by a regenerative shock absorber is in the range of 10s of W to 1000s of W (e.g. [24]-[26]). It can be used for controlling vehicle vibration (e.g. [27]) or structural vibration in the form of a seismic monitoring and protection system [28]. Solar-powered vehicles, as self-powered dynamic systems, exploit renewable energy as a power source in a self-sustained scheme. Examples of some recent developments in this area include Multibody Advanced Airship for Transport (e.g. [29]-[31]), and Brunel Solar-powered Airships ([5], [32], [33]).

Self-powered systems have attracted much attention recently. Many novel self-powered devices have been developed with application in dynamic systems and various other systems. Examples and applications of some recent self-powered systems include, a maximum power direction tracking system for maximizing the harvested energy of solar panels [34], vanadium neutron detectors [35], functional triboelectric generator as a vibration sensor or active sensor [36], wastewater treatment system [38], nonlinear harvester with a bistable generator [39], autonomous bio-sensing actuator [40], glucose sensor [41], self-powered contact area and eccentric angle sensors [42], metal surface anti-corrosion protection system using energy harvested from rain drops and wind [43], cleaning of air pollution by wind driven triboelectric nanogenerator [44], barcode based on sliding electrification identification systems [45], rotation sensor based on electrification at rolling interfaces for multi-tasking motion measurement system [46], ultra sensitive cytosensor [47], seawater desalination and electrolysis [48], and ultrasensitive pressure sensing system [49].

In the present paper, a combined representation of regenerative and renewable energy exchange in the development of a self-powered dynamic system is provided. A rigorous framework that explores the energy supply and demand for a self-powered dynamic system, while considering uncertainties, is developed in the context of Optimal Uncertainty Quantification [50], for the first time. The feasibility of developing fully self-powered systems is investigated as a generalized approach, through numerical examples for dynamic systems with feedback control.

The organization of the paper is as follows. The concept of self-powered dynamic systems is presented. Renewable and regenerative energy exchange is formulated, and non-dimensional power parameter is investigated for self-powered dynamic systems. Dynamics and power for such systems is formulated in the framework of Optimal Uncertainty Quantification (OUQ), and uncertain parameters and optimal bounds are discussed. An example of self-powered vibration control is presented, and the conditions for self-sustainability of a system in terms of the input energy requirement are explored.

Self-powered Dynamic Systems

Fig. 1 represents a regenerative multibody dynamic system with actuators (motors denoted by M) or generators (denoted by G) subjected to mechanical excitations and other forms of energy input. The “MG” components act as both actuators and generators through a regenerative mechanism (or energy transfer) such as electromagnetic, piezoelectric, and electrostatic schemes.

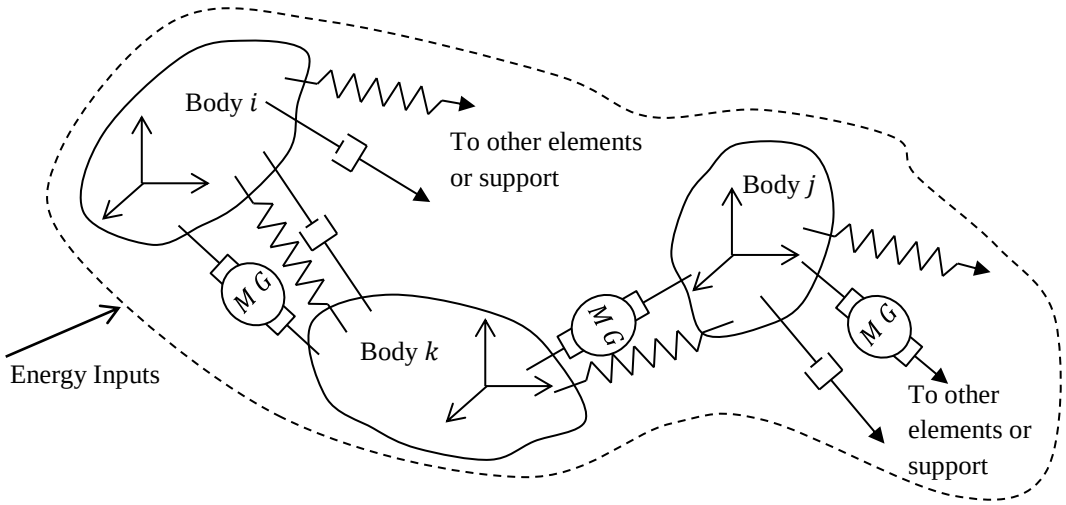

Fig. 1 A regenerative multibody dynamic system with motors and generators and energy inputs.

Fig. 2 shows a regenerative electromechanical system and a solar-powered vehicle as examples of self-powered dynamic systems. The energy regeneration may power a vibration control system [1]-[6] in: a road vehicle with active suspension, aerial vehicle structures (e.g., wing vibration control of an aircraft), civil structures (e.g., structural vibration control for seismic safety), and so on. A solar-powered aerial vehicle (e.g., Brunel solar-powered airship [5], [29]-[33]) is a self-powered dynamic system, which uses renewable energy as the power source for the vehicle duty cycles. This concept is applicable to aerial, space and road vehicles. A solar-powered airship benefits from the buoyancy force, which assists in lowering the energy consumption associated with maintaining the vehicle in the air (particularly in the hovering mode) which is an advantage. Energy regeneration is also possible by kinetic energy recovery in a descending electric aerial vehicle where the propellers of the electric motors are used for both propulsion, and energy generation (as a wind turbine in descending).

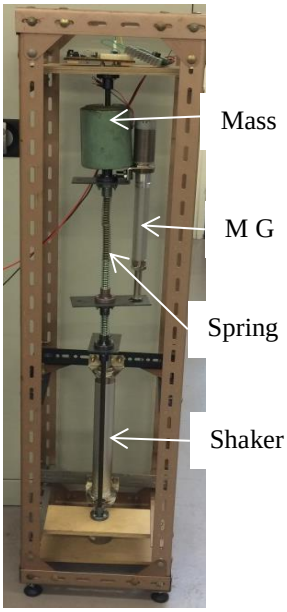

(a) A regenerative electromechanical system

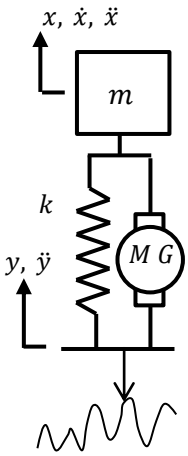

(b) A schematic of the regenerative system

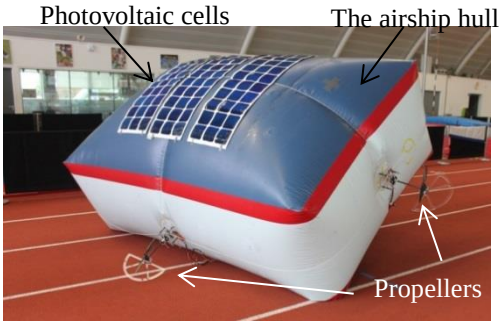

(c) A solar-powered aerial vehicle

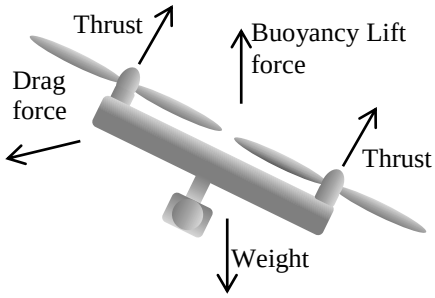

(d) A free-body diagram of the airship

Fig. 2 Examples of self-powered dynamic systems

The development of regenerative and renewable self-powered systems is presented in the next sections.

Regenerative and renewable energy exchange in dynamic systems

The equations of motion of a multibody system shown in Fig. 1, with actuation, and subjected to excitation inputs, and/or other forms of force or energy inputs may be written as

$$[M]\{\ddot{x}\} + [c]\{\dot{x}\} + [k]\{x\} = \{f_{act.}\} + \{f_{ext.}\} + \{f_{ren.}\} \quad (1)$$

where $[M]$, $[c]$, and $[k]$ are the mass, damping and stiffness matrices, respectively, $\{x\}$, $\{\dot{x}\}$ and $\{\ddot{x}\}$, are the displacement, velocity and acceleration vectors, respectively, $\{f_{act.}\}$ denotes the actuation forces (e.g., electric motors or other actuators), $\{f_{ext.}\}$ is the external force vector (due to other excitations), and $\{f_{ren.}\}$ represents the equivalent external forces generated due to renewable energy inputs (e.g., solar energy) and/or regenerative forces realized by converting excessive kinetic energy to useable input energy (e.g., electrical energy generated by an electric generator in the system).

A renewable energy source and a regenerative actuation system with the corresponding electrical circuit is illustrated in Fig. 3 for a dynamic system. In this figure the dynamic system is assumed as an equivalent single degree of freedom mass-spring-

damper with input base excitation, $\ddot{y}$, and external force input, $f(t)$. This system is used in analysing the self-powered system.

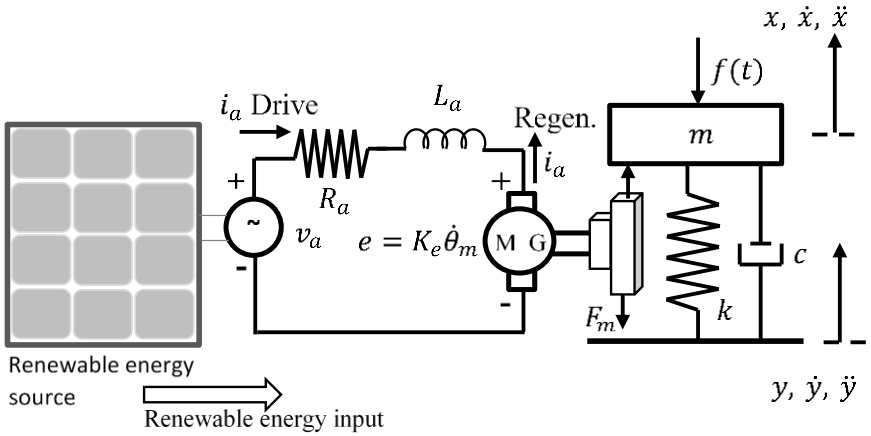

Fig. 3 A schematic for a self-powered dynamic system with renewable energy input and a regenerative system.

A more detailed presentation of this system (Fig. 3) is given in Fig. 4. This system includes an equivalent circuit of a photovoltaic cell for the renewable energy source and a control schematic for the actuation and the regenerative system.

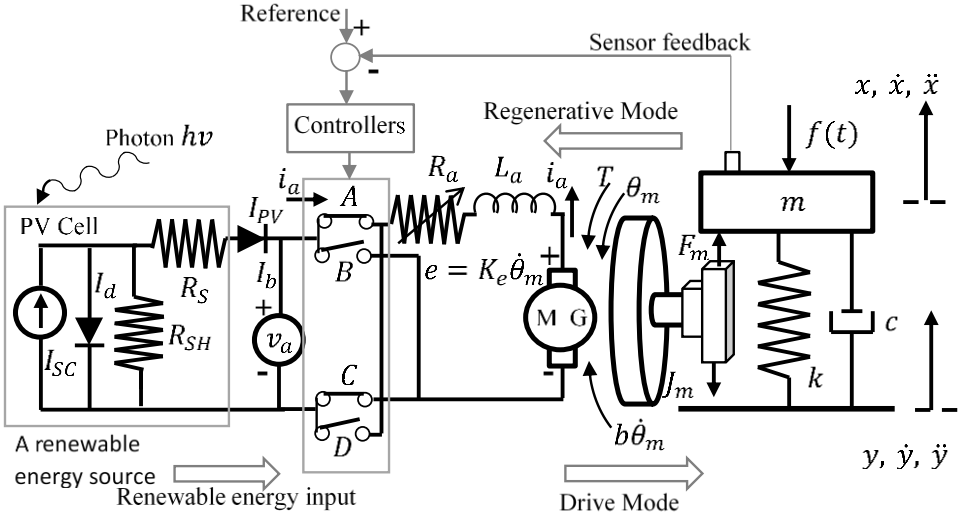

Fig. 4 A self-powered dynamic system with renewable energy input and regenerative actuation.

The equation of motion of mass, m, in Fig. 4 is given by

$$F_m - f(t) + c(\dot{x} - \dot{y}) + k(x - y) = m\ddot{x} \quad (2)$$

This formulation can be modified for each specific case. For instance, for the solar-powered airship in Fig. 2(c), the motion of the base excitation, stiffness, and damping can be ignored if required (internal stiffness of the blimp relative to the propellers can still be

considered), and the actuator force may represent the propulsion force of the propellers applied to the aerial vehicle.

For regenerative cases as in Fig. 2(a) and (b) (e.g., applications to self-powered vibration control), the equation of motion of mass, m, in Fig. 4 may be expressed by

$$m\ddot{z} + c\dot{z} + kz = -m\ddot{y} + F_m - f(t) \tag{3}$$

where $\ddot{y}$ denotes the acceleration excitations to the system. The relative displacement of the mass, m, with respect to the base is $z = x - y$, where x is the absolute displacement of m. Also, $f(t)$ is the external force, F_m is the actuator force generated by the motor, k is the stiffness, and c represents the damping coefficient. It is assumed that the conversion of torque, T, to linear force, F_m, for the motor/actuator can be given by $F_m = \varphi T$ (φ takes into account the lead/roller/ball screw, rotary to linear gear ratio, and efficiency).

The equation of motion for the motor can be written as

$$J_m\ddot{\theta}_m + b_m\dot{\theta}_m = K_t\, i_a \tag{4}$$

where J_m is the moment of inertia of the rotor and $b_m$is the coefficient of viscous friction. The applied torque to the rotor, T, in terms of the armature current, i_a, can be given by $T = K_t\, i_a$, where K_t is the torque constant of the motor. The back-electromotive force (back-emf) voltage, e, in terms of the rotational velocity, $\dot{\theta}_m$, of the shaft is given by $e = K_e\, \dot{\theta}_m$, where K_e is the electric constant (voltage constant) of the motor and $\dot{z} = \dot{\theta}_m/\varphi$ may represent the rotary to linear motion relationship. It should be noted that if piezoelectric or electrostatic energy conversion mechanisms are used, instead of a motor/generator, the electromechanical relationships for velocity/voltage and force/current can be modified accordingly, for taking into account the corresponding mechanism.

The equation for the electric circuit of the motor can be expressed by

$$L_a\frac{di_a}{dt} + R_a i_a = v_a - K_e\dot{\theta}_m \tag{5}$$

If the relative effect of inductance, L_a, is negligible (Note: This is in fact the “leakage” inductance, which is relatively small in a good motor) compared to the effect of the resistance, then

$$R_a i_a = v_a - K_e\dot{\theta}_m \tag{6}$$

When the motor operates as a generator, Equation (6) can be written as

$$e = v_a + R_a i_a \tag{7}$$

where $e = K_e\, \dot{\theta}_m$. In a DC linear motor the relation between the force and velocity in terms of the motor parameters may be expressed by

$$e = K_e\, \dot{\theta}_m;\; e = K_e\, \varphi\dot{z} \tag{8}$$

The torque and the force can be obtained as

$$T = K_t\, i_a;\; F_m = \varphi K_t\, i_a \tag{9}$$

For a DC motor, $K_t = K_e$ in consistent units (SI), assuming accurate energy conversion. In order to generate the force, F_m, the consumed power by the voltage source can be determined by substituting Equations (8) and (9) into (6) as

$$v_a = \frac{R_a F_m}{\varphi k_t} + k_e\varphi\dot{z} \tag{10}$$

The required force can be calculated by rearranging Equation (10) as

$$F_m = \varphi k_t \frac{v_a - k_e \varphi \dot{z}}{R_a} \tag{11}$$

The consumed/required power can be obtained from Equations (9) and (10) as

$$P_c = v_a i_a = \left(\frac{R_a F_m}{\varphi k_t} + k_e \varphi \dot{z}\right) \frac{F_m}{\varphi k_t} \tag{12}$$

If the equivalent damping constant for the motor is taken as the coefficient of velocity, $\dot{z}$, in the force equation, an expression can be extracted from Equation (11) as (when $K_t = K_e$)

$$c_{eq} = \frac{\varphi^2 {k_t}^2}{R_a} \tag{13}$$

Note that in the regenerating mode, when the motor is used as a generator, the equivalent damping can be written as (if (7) is written as $e = R_B i_a + R_a i_a$)

$$c_{eq} = \frac{\varphi^2 {k_t}^2}{R_a + R_B} \tag{14}$$

where R_B corresponds to the equivalent electrical load of the battery due to the generator back-emf in the charging mode where $v_a = R_B i_a$.

The consumed power can be determined by

$$P_c = v_a i_a = \frac{{F_m}^2}{c_{eq}} + F_m \dot{z} \tag{15}$$

The parameter μ is defined as (for $\dot{z} \neq 0$) [1]-[3] and [21]

$$\mu = \frac{F_m}{-c_{eq} \dot{z}} \tag{16}$$

by substituting μ in the power consumption equation in (15). Then, the equation for P_c can be rewritten as

$$P_c = c_{eq} \dot{z}^2 \mu(\mu - 1) \tag{17}$$

A dimensionless form of power, P_{dm},may be given by $P_{dm} = P_c / c_{eq} \dot{z}^2$. Then, it is seen from (17) that for $0 < \mu < 1$ we have $P_{dm} < 0$. Therefore for this range of μ the power consumption is negative, which indicates that the regenerative actuator functions as a generator. P_{dm} may be used when the changes of non-dimensional power is desired with respect to the mechanical parameters (i.e., velocity and equivalent damping).

By taking into account the power received from renewable energy, i.e. the photovoltaic cells (PV cells) here (Fig. 4), the total power consumption may be given by

$$P_c = v_a I_b = v_a(\alpha i_a - I_{PV}) \tag{18}$$

The total power consumption in Equation (18) can be expressed in terms of the electromechanical parameters as

$$P_c = \left(\frac{R_a F_m}{\varphi k_t} + k_e \varphi \dot{z}\right)\left(\alpha \frac{F_m}{\varphi k_t} - I_{PV}\right) \tag{19}$$

Here $\alpha = 1$ corresponds to the Drive Mode, and $\alpha = -1$ for the Regenerative Mode of the actuator. If α is set to the fixed value of -1, the regenerative actuator functions only as a generator.

The current-voltage characteristics of PV cells may be expressed by the following relation, for the equivalent PV circuit shown in Fig. 4:

$$I_{PV} = I_{SC} - I_d - I_{SH} \tag{20}$$

where I_{PV} is the current applied to the load in the PV circuit, I_{SC} is the short circuit current, and I_d is the diode current (leakage currents arise). The equation for I_{PV} in (20) can be written in terms of the expressions of I_d and I_{SH} as

$$I_{PV} = I_{SC} - I_0(\exp(q(v_a + I_{PV}R_s)/nk_BT_c) - 1) - (v_a + I_{PV}R_s)/R_{SH} \quad (21)$$

where R_{SH} is a parallel shunt resistance (Fig. 4), I_{SH} is the current through the shunt resistor R_{SH}, I_0 is the reverse (dark) saturation current (the leakage current in the absence of light), q is the electron charge (1.602×10^{-19} C), and v_a is the voltage across the diode. The voltage drop in the electrical contacts is modeled as series resistance R_s. Also, k_B is Boltzmann's constant (1.381×10^{-23} J/K), T_c is the junction temperature (K), and n is the ideality factor with n=1 for an ideal diode. The ideality factor varies from 1 to 2 depending on the fabrication process and the semiconductor material. An example of current-voltage (I-V) and power-voltage (P-V) curves for direct sun radiation to a 2 m^2 of monocrystalline semi flexible silicon solar panels with 22.5% efficiency for the PV cells is given in Fig. 5 (The specifications for the PV cells in the figure are, SunPower Maxeon with size: 125mm x125mm; power output: 3.42 watts, for 5.93A current and 0.58V voltage; Weight: 7g).

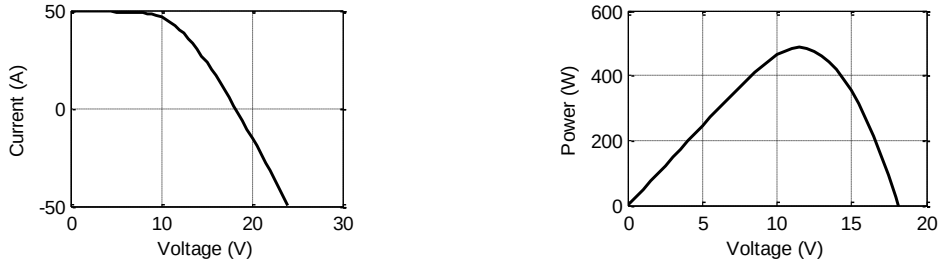

Fig. 5 I-V and P-V curves for a PV cell.

From equations (6), (8) and (18) the power may also be expressed in the form:

$$P_c = (R_a i_a + e)(\alpha i_a - I_{PV}) \quad (22)$$

By expanding the equation we get

$$P_c = R_a \alpha i_a^2 + e\alpha i_a - R_a i_a I_{PV} - eI_{PV} \quad (23)$$

Using $\sigma = -R_a i_a / e$, the power can be expressed as (Note: The negative sign for σ is used to indicate the transition from motor to generator as given in equations (6) and (7))

$$P_c = \frac{e^2}{R_a}\alpha\sigma(\sigma - 1) + \sigma e I_{PV} - eI_{PV} = \frac{\alpha e^2}{R_a}\sigma^2 - \left(\frac{\alpha e^2}{R_a} - eI_{PV}\right)\sigma - eI_{PV} \quad (24)$$

Defining $a = \frac{e^2}{R_a}$, and $b = eI_{PV}$, the power equation can be written as

$$P_c = a\sigma^2 - (a - b)\sigma - b \quad (25)$$

With $\gamma = a/b$, a dimensionless expression for power, $P_{d\gamma}$, is given by

$$P_{d\gamma} = P_c/(eI_{PV}) = \gamma\sigma^2 - (\gamma - 1)\sigma - 1 \quad (26)$$

This non-dimensional power, $P_{d\gamma}$, is obtained with respect to the electrical current of PV, and the back-electromotive force (back-emf) voltage, e. The plot of the dimensionless power, $P_{d\gamma}$, in Equation (26) is shown in Fig. 6 for γ=0.4, 0.5, 2, 2.5.

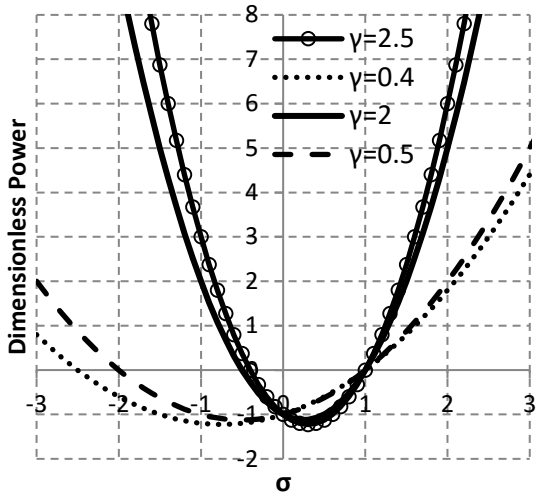

Fig. 6 Non-dimensional power, $P_{d\gamma}$, $\gamma = a/b$

Fig. 6 shows that for $-\frac{1}{\gamma} < \sigma < 1$, the power consumption is negative, which corresponds to power generation by the regenerative system and the supplied renewable energy. It shows how the energy generation band can be expanded in correspondence with the inverse of γ, which is in direct relation to the increase in the current generated by the PV cells, eI_{PV}, for a constant value of $\frac{e^2}{R_a}$. The maximum value of power generation for each γ value may be calculated as $\sigma = \frac{\gamma-1}{2\gamma}$. Note that for $\sigma = 1$, the power is zero. This means that the generated power is equal to the consumed power by the actuator. The dimensionless power, $P_{d\gamma}$, is also plotted with respect to σ and γ in Fig. 7. This figure is the generalized form of the plot in Fig. 6.

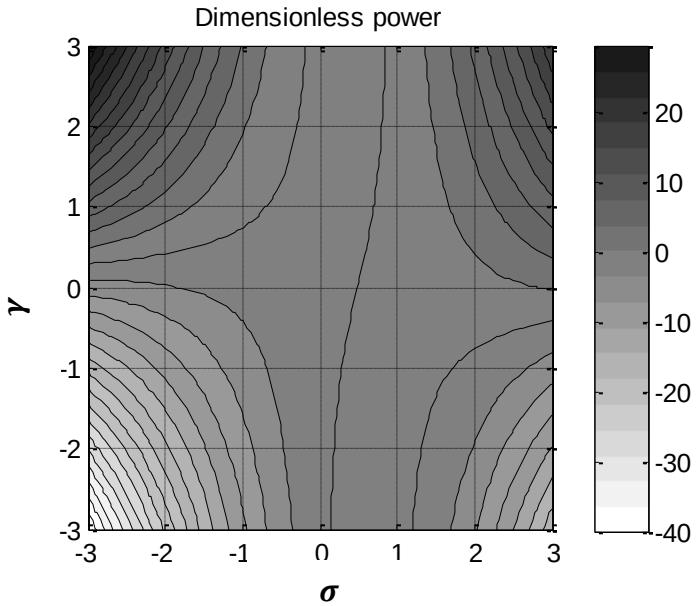

Fig. 7 Non-dimensional power, $P_{d\gamma}$, versus σ and γ

For $\lambda = b/a$, the non-dimensional expression for power, $P_{d\lambda}$, may be expressed by

$$P_{d\lambda} = P_c/(e^2/R_a) = \sigma^2 - (1-\lambda)\sigma - \lambda \quad (27)$$

This non-dimensional power, $P_{d\lambda}$, is obtained with respect to the back-emf, e, and resistance R_a. The plot of the non-dimensional power, $P_{d\lambda}$, in Equation (27) is shown in Fig. 8, for λ =0.4, 0.5, 2, 2.5.

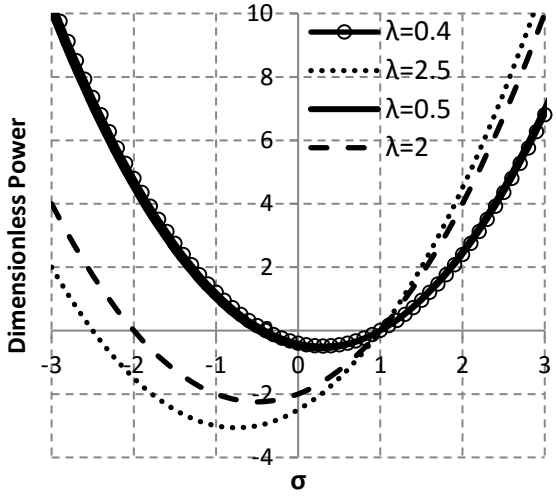

Fig. 8 Non-dimensional power, $P_{d\lambda}$, $\lambda = b/a$

Fig. 8 shows that for $-\lambda < \sigma < 1$, the power consumption is negative, which corresponds to generating. The energy generation band can be expanded by increasing the value of λ, by increasing in the current generated by the PV cells, eI_{PV} (when $\frac{e^2}{R_a}$ is kept constant). The maximum value of power generation for each λ value can be calculated as $\sigma = \frac{1-\lambda}{2}$. This non-dimensional power, $P_{d\lambda}$, is also plotted with respect to σ and λ in Fig. 9. This figure shows the generalized form of the plot in Fig. 8.

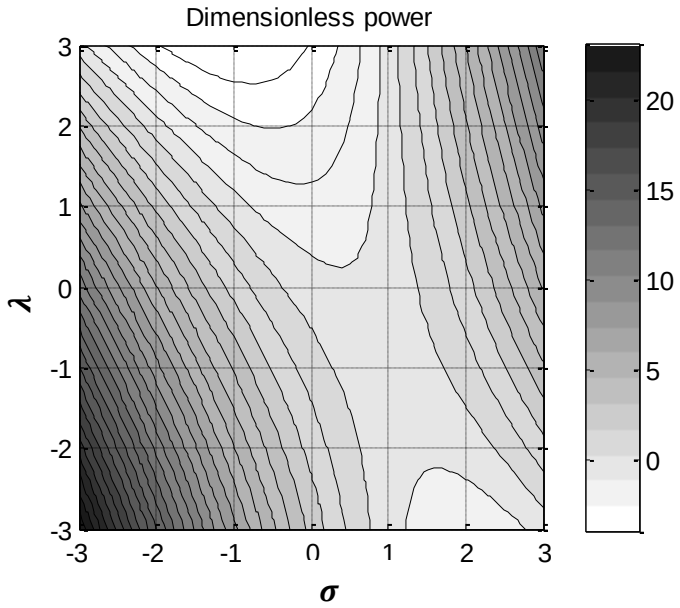

Fig. 9 Non-dimensional power, $P_{d\lambda}$, versus σ and λ

Although $P_{d\gamma}$ and $P_{d\lambda}$ can be used interchangeably, $P_{d\gamma}$, may be a more convenient way to express the non-dimensional power when I_{PV} is a constant.

Fig. 6 to Fig. 9 show the result of energy exchange with regard to consumption and generation of energy for a dynamic system with regenerative and renewable energy inputs. In a self-powered system, it is required that the total energy generation is equal or larger than the total energy consumption at any time. The generated power (e.g., when P_d is negative), should provide the desired actuation/motion (e.g., F_m, as the term responsible for power consumption) for the system while considering the input energy and input excitations to the system (e.g., I_{PV}, $\ddot{y}$, $f(t)$, F_m). The system inputs/outputs, I_{PV}, $\ddot{y}$, $f(t)$, F_m, P_c, are usually constrained and uncertain. Analysis of the self-powered system in the presence of uncertainty is discussed in the next section as a constrained optimization problem in the framework of Optimal Uncertainty Quantification.

Optimal uncertainty quantification for self-powered systems

A framework that explores energy supply and demand for a self-powered dynamic system, while considering uncertainties and the optimal bounds, is proposed now. Optimal Uncertainty Quantification (OUQ) [50] is used here to take into account uncertainty measures with optimal bounds, and incomplete information about the energy inputs to the dynamic system and response function. The self-powered dynamic system theory is formulated in the framework of OUQ as a well-defined optimization problem corresponding to extremizing the probabilities of system failure with respect to the required energy supply subject to the imposed constraints. The input energy and the excitations to a self-powered system (e.g., I_{PV}, $\ddot{y}$, $f(t)$, F_m) are usually constrained and uncertain. The input energy is required to provide the desired actuation/motion (e.g., F_m) for the system. There exist bounded ranges of the input parameters to the system, while the output is also constrained according to the desired performance of the system. The

desired performance can be defined in terms of displacement, velocity and acceleration (e.g., z, $\dot{z}$, $\ddot{x}$) of the system. In order to consider this constrained and uncertain problem for the input and the output, the energy exchange for the dynamic systems is formulated in the OUQ framework, as presented below.

The available net power is determined by subtracting the total of consumed power, P_c, by the actuator and the resistor energy loss, from the recoverable (generated) power by the generator. Therefore, the available net power is given by P_g - P_c - $R_a {i_a}^2$. A self-powered control is achievable if $P_g \geq P_c + R_a {i_a}^2$.

If $P_T = P_c + R_a {i_a}^2$, assume $P_c: \mathcal{X} \to \mathbb{R}$, $X \to P_c(X)$, with the probability of $\mathbb{P} \in \mathcal{M}(\mathcal{X})$, where X and $\mathcal{X}$ denote the deterministic and the stochastic forms of the inputs, respectively. In a stochastic representation of a self-powered system, we require that the probability of the power consumption function, $P_c(X)$ being larger than the power generation, P_g, (i.e. the self-powered scheme to fail) is less than ϵ. This can be written as (where the net power is $P_g - P_T$)

$$\mathbb{P}\left[P_T(X) \geq P_g\right] \leq \epsilon \tag{28}$$

Assume that the probability function is a member of admissible extremal scenarios $\mathcal{A}$ (or $(P_c,\ \mathbb{P}) \in \mathcal{A}$), where $\mathcal{A}$ is defined as

$$\mathcal{A} := \left\{ (p_c, \mu) \middle| \begin{matrix} p_c: \mathcal{X}_1 \times \cdots \times \mathcal{X}_n \to \mathbb{R} \\ \mu = \mu_1 \otimes \mu_2 \otimes \cdots \otimes \mu_n \\ \mathbb{E}_\mu[p_T] \leq P_{max} \end{matrix} \right\} \tag{29}$$

Here n denotes the number of inputs, for inputs $\mathcal{X}_i$, $i = 1, \cdots, n$, $\mathbb{E}_\mu[p_T]$ is the bounded mean output power, μ_i is the probability measure of the input parameter $\mathcal{X}_i$ ($\mu_i \in \mathcal{P}(\mathcal{X}_i)$), and p_c is a possible output function of P_c for the corresponding inputs/parameters $\mathcal{X}_i$. The original problem entails optimizing over a collection of (p_c, μ) that could be $(P_c, \mathbb{P})$. P_{max} is the output upper bound, if known. $\mathcal{X}_i$ and μ_i parameters can be constrained values with corresponding lower and upper bounds for each i.

The optimal bounds on the probability of power consumption according to the required performance can be described by the upper bound, $\mathcal{U}(\mathcal{A})$ as

$$\mathcal{U}(\mathcal{A}) := \sup_{(p_c,\mu)\in\mathcal{A}} \mu\left[p_T(X) \geq P_g\right]$$

and the lower bound, $\mathcal{L}(\mathcal{A})$, corresponding to the minimum required power consumption can be stated as

$$\mathcal{L}(\mathcal{A}) := \inf_{(p_c,\mu)\in\mathcal{A}} \mu\left[p_T(X) \geq P_g\right]$$

These give the optimal bounds as

$$\mathcal{L}(\mathcal{A}) \leq \mathbb{P}\left[P_T(X) \geq P_g\right] \leq \mathcal{U}(\mathcal{A}) \tag{30}$$

The power consumption can be determined by solving the constrained optimization problem for extremal scenarios $\mathcal{A}$, with the inputs/parameters are also constrained. If I_{PV}, $\ddot{y}$, $f(t)$, F_m are considered as the input to the system, then

$$I_{PV} \in \mathcal{X}_1 := [0, I_{max}]\ \text{Amp},$$
$$\ddot{y} \in \mathcal{X}_2 := [0, \ddot{y}_{max}]\ \text{m/s}^2,$$
$$f(t) \in \mathcal{X}_3 := [0, f_{max}]\ \text{N},$$
$$F_m\ \in \mathcal{X}_4 := [0, F_{max}]\ \text{N},$$
$$k_p \in \mathcal{X}_5 := \left[0, k_{p,max}\right],\ k_d \in \mathcal{X}_6 := \left[0, k_{d,max}\right],\ k_i \in \mathcal{X}_7 := \left[0, k_{i,max}\right],$$

where k_p, k_d, and k_i are the feedback controller parameters, which for a PID controller correspond to proportional, derivative, and integral terms. In a three-dimensional motion each of the physical parameters $\ddot{y}$, $f(t)$, F_m can be considered as vectors with independent $\mathcal{X}$ constraints for each motion direction. Therefore three independent $\mathcal{X}$ values can be considered for each vector. The power consumption output depends on the desired performance and can be defined as a function of displacement, velocity and/or acceleration (e.g., z, $\dot{z}$, $\ddot{x}$) of the system, where these performance parameters can considered as constrained values (e.g., $a_{min} \leq \ddot{x} \leq a_{max}$). Therefore $\mathcal{A}$ may be given by

$$\mathcal{A} \coloneqq \left\{ (p_c, \mu) \middle| \begin{matrix} p_c \colon \mathcal{X}_1 \times \mathcal{X}_2 \times \mathcal{X}_3 \times \mathcal{X}_4 \times \mathcal{X}_5 \times \mathcal{X}_6 \times \mathcal{X}_7 \to \mathbb{R} \\ \mu = \mu_1 \otimes \mu_2 \otimes \mu_3 \otimes \mu_4 \\ \mathbb{E}_\mu[p_T] \leq P_{max} \end{matrix} \right\} \tag{31}$$

The optimization cost function can include multiple parameters. For example, it can include the consumed power and the power loss plus the output displacement, velocity, or acceleration (e.g., z, $\dot{z}$, $\ddot{x}$) to be optimized.

In the analysis of a solar-powered airship (Fig. 2), as a self-powered dynamic system, the parameters can be assigned as $\ddot{y} = 0$, I_{max} for the maximum current generated by the solar cells, f_{max} as the maximum aerodynamic load (which may include any other load applied by any external energy source; e.g., muscle force in human powered systems), and F_{max} as the maximum thrust generated by the propellers. For a regenerative system, I_{PV} can exist if photovoltaics are used (e.g., solar-powered ground vehicles with regenerative suspension), where $\ddot{y}$ translates to the acceleration base excitations (e.g., due to a vehicle travelling on a road, or seismic load excitations to a structure), $f(t)$ can be interpreted as external forces (e.g., aerodynamic loads, if exist), and F_{max} is the maximum force that the regenerative actuator is required (for example, for a self-powered vibration control scheme).

If (experimental) sample data is available then the OUQ can be generalized to the Machine Wald [51] technique which is equivalent to performing Bayesian inference but optimizing the prior. In Machine Wald, if an estimation of a function $\Phi(\mu)$, is function θ of sample data d, then the estimation error $\theta(d) - \Phi(\mu)$ is required to be equal to zero. Examples of the feasibility of developing fully self-powered dynamic systems are discussed in the next section.

Self-powered dynamics and control

A self-powered system is analyzed in this section as an example. The system illustrated in Fig. 4, which can represent the physical systems shown in Fig. 2, is considered for the analysis. The study of the system for self-powered capability is discussed. In particular, self-powered actuation is explored for feedback control of the system. Three different excitations: step, sinusoidal, and random, are considered as the inputs to the system. The response of the system is observed using a sensor (Fig. 4). Specifically, the response is considered as the acceleration of the mass, and an LVDT (linear variable differential transformer/transducer) is used to monitor the response. The control task is to reduce the displacement (or acceleration, or velocity depending on the application) of the mass to an acceptable level, using the actuation force, while the actuator(s) draw the self-

generated power in the system. A PID (proportional-integral-derivative) controller is used in this example with a proportional gain of k_p= 859.4, derivative gain of k_d=610, and an integral gain of k_i=92.1. These PID coefficients are chosen to provide an acceptable performance for the system (i.e., to reduce the displacement/acceleration output to an acceptable level in the present example).

The level of input excitations and the acceptable performance serve as the constraints for the OUQ framework in this example. The parameter values of the system are: mass m=280 kg, spring stiffness k=16000 N/m, and the equivalent damping coefficient c=423 Ns/m. The equivalent damping is the damping produced by the resistor and the battery load due to the generator back-emf in the electrical circuit of Fig. 4, as given by Equation (14). This equivalent damping can serve as a mechanical viscous damper, which is a passive controller, to control the system response. Equations (2) and (3) are used to obtain the response of the system. The single motor/generator regenerative system in Fig. 4 will control the motion in the actuator mode and produce power when performing as a generator. A switching circuit (e.g., the switches AC and BD in Fig. 4) is used to switch between the motor and generator functions. The switching logic strategy is based on the level of acceptable performance of the system. If the acceptable performance is not satisfied (e.g., displacement or acceleration is larger than the performance threshold) then the switch allows actuation only, until satisfactory performance is achieved through the actuator control force F_m. A suitable control strategy (e.g., PID, fuzzy logic, etc.) may be used to control the actuation force. If the performance level is satisfied then the regenerative system is switched into the generator mode and the produced power is stored in the battery (Fig. 4). The block diagram of such controller can be represented as in Fig. 4 where the motion in the dynamic system (i.e., the motion of the mass) is measured and used in feedback for the controller. The power consumed by the actuator, P_c, for producing the force F_m, is given by $F_m \times \dot{z}$. The power generated by the regenerative system is obtained by the force applied to the generator (due to the kinetic energy of the mass) multiplied by the velocity $\dot{z}$.

This problem can be expressed by Equation (28) in the OUQ framework as $\mathbb{P}\left[P_T(X) \geq P_g\right] \leq \epsilon$, where P_T is the total consumed power (i.e., $P_T = P_c + R_a {i_a}^2$) in the system, and P_g denotes the generated power when the motor is in the generator mode. The OUQ problem requires that: *the probability of the total consumed power is greater than the generated power (i.e., failure of the system to provide a positive net power), should be smaller than ϵ, while satisfying optimal bounds*. In the following problem $\epsilon = 0$ (i.e., $p_T(X) < P_g$ is desired). The optimal bounds in this problem can be expressed as $\ddot{y} \in \mathcal{X}_1 := [0, \ddot{y}_{max}]$ m/s^2 (i.e., the input acceleration amplitude), $F_m \in \mathcal{X}_2 := [0, F_{max}]$ N, where F_{max} denotes the maximum force that can be generated by the actuator). It is possible to provide an acceptable range for the PID control parameters (i.e., $k_p \in \mathcal{X}_3 := \left[0, k_{p,max}\right]$, $k_d \in \mathcal{X}_4 := \left[0, k_{d,max}\right]$, $k_i \in \mathcal{X}_5 := \left[0, k_{i,max}\right]$). The admissible set $\mathcal{A}$, is given by

$$\mathcal{A} := \left\{ (p_c, \mu) \middle| \begin{matrix} p_c: \mathcal{X}_1 \times \mathcal{X}_2 \to \mathbb{R} \\ \mu = \mu_1 \otimes \mu_2 \\ \mathbb{E}_\mu[d] \leq d_{max} \\ p_T(X) < P_g \end{matrix} \right\}$$

where d_{max} is the maximum acceptable output displacement. In this problem d is calculated and is minimized while the condition $p_T(X) < P_g$ is satisfied for various PID parameters. In fact, the bounds are not computed in the example in this section (the framework is only presented at a conceptual level). The results for an acceptable d, and $p_T(X) < P_g$condition corresponding to various PID parameters and actuator force, F_m, are discussed next (the actuator force is not optimized in this example, and is discussed in the following examples).

Note that the generated power is determined only during the time that the controller is off and the switching logic provides the generator function. Also, the consumed actuation power is determined only while the switching logic allows the controller to provide actuation.

In the present example a sinusoidal excitation is applied to the system (Fig. 4). Suppose that a self-powered control condition is required for the system, with an input acceleration amplitude of 0.39 (i.e., $\ddot{y}_{max}$=0.39), or we have $\ddot{y} = 0.39 \sin \omega t$, and an excitation frequency of $\omega = 2\pi$. A PID controller, with the parameters given before, is used in this example. It is found that the PID controller reduces the output relative displacement by about 16% (from 0.022m to 0.019m), which is considered to be an acceptable performance in this example (Fig. 10(a)).

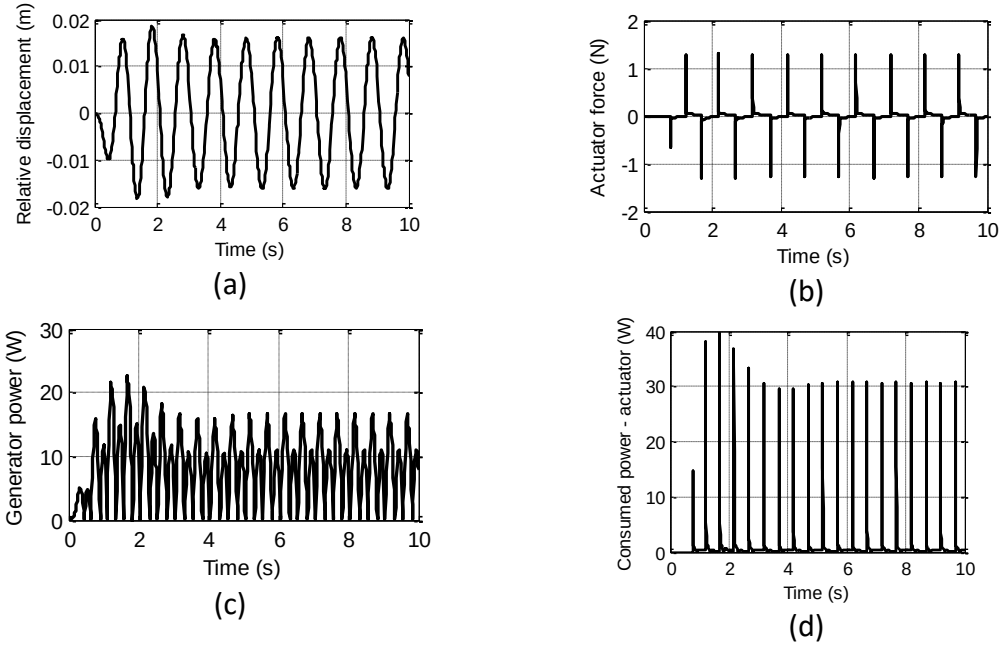

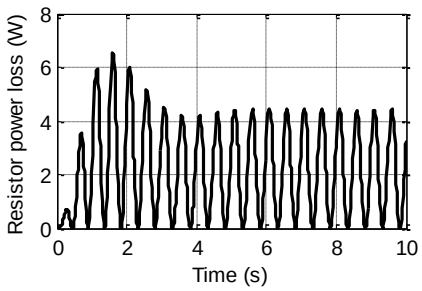

(e)

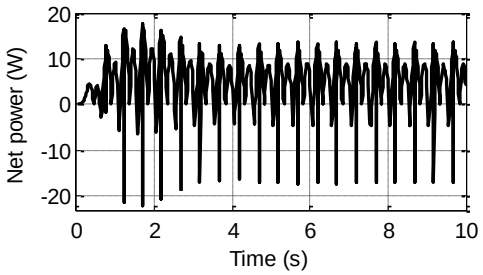

(f)

Fig. 10 (a) Relative displacement, (b) Actuator force, (c) Power produced by the generator, (d) Power consumed by the actuator, (e) Resistor power loss, (f) Available net power.

The results in Fig. 10 show that self-powered actuation is feasible for providing a relative displacement with amplitude 0.019m (Fig. 10(a)). This is due to the available positive net power, as shown in Fig. 10(f). Therefore, the system is able to control the motion of the mass and use the generated power in the system in a self-powered scheme. However, there is a limit for the control level of the output acceleration and the required force in achieving self-powered control. The limits can be investigated in the OUQ framework, which deals with the constrained optimization problem. The following example studies these limits and constraints.

In order to investigate the control limits, the PID controller parameters are changed and the simulation is repeated for each controller parameter set. As the proportional gain is the term responsible for the response and the agility of the system in suppressing the output (displacement, acceleration and/or velocity), this parameter has been chosen and scaled corresponding to various control parameter sets. The derivative and integral parameters of the controller are updated according to the same scaling factor as the proportional gain. The PID controller parameters given above are scaled by a factor of 0.01 and 10 separately, and the simulation in Fig. 10 is repeated. The resulting displacement response of the system is shown in Fig. 11. Parameter options 1, 2, 3 in Fig. 11 correspond to the scale factors of 0.01, 1 and 10, respectively, for the PID parameters. Fig. 11 shows how the scaling of the controller parameter from 0.01 to 10 can suppress the output displacement level at the cost of increasing the required control actuation force.

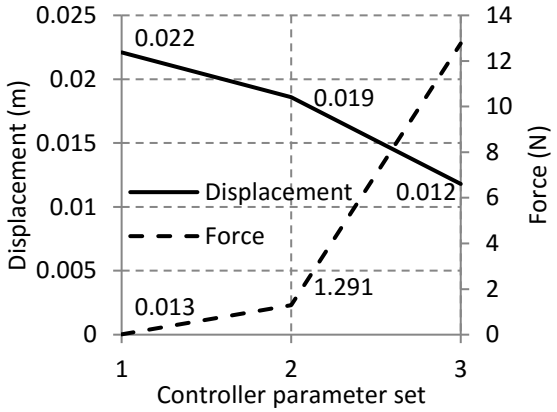

Fig. 11 Displacement of the system for 3 different control parameter sets, and the corresponding control force.

The power consumed by the actuation force for maintaining the output displacement level is plotted in Fig. 12(a), together with the amount of power generated by the regenerative system. The total available net power corresponding to each controller parameters set is plotted in Fig. 12(b). RMS (root mean square) of the power values are used in the plots. The available net power is equal to the power generated by the generator minus the sum of the power consumed by the actuator and the power loss of the resistor.

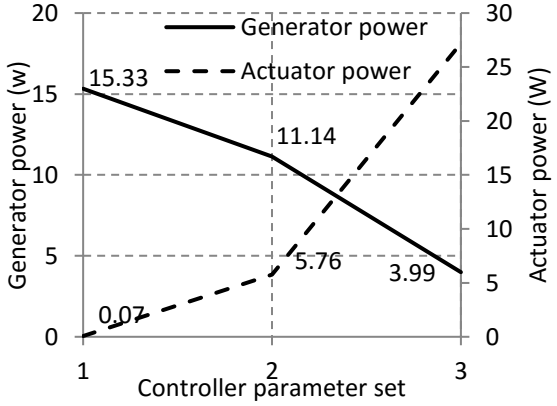

(a)

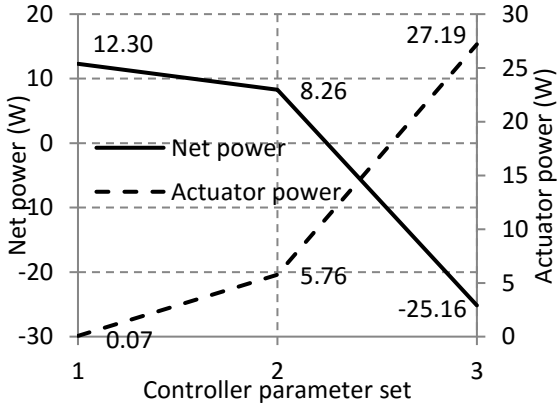

(b)

Fig. 12 (a) Generator power and consumed actuator power for different controller parameter sets, (b) Total available net power for different controller parameter sets.

As shown in Fig. 12, the system is capable of providing self-powered control force by the actuator for the control parameter sets 1 and 2 (corresponding to PID scaling factors of 0.01 and 1). The self-powered control is achievable as the available net power is positive. However, in the control parameter option 3 (corresponding to a PID scaling factor of 10), the self-powered control is not feasible as the available net power is negative, or the consumed power for actuation force plus the power loss in the system is more than the generated power in the system. Note that if the system is used only as an energy harvester, the required power by the actuator is zero as there will be no active control. The control in this case will be only a passive control system due to the resistor equivalent damping and the battery load due to the generator back electromotive force.

Next, a similar procedure is applied with other input excitations. In the following example, the response of the system to a step input with $\ddot{y}$=0.4 m/s^2 ($\ddot{y}_{max}$=0.4 m/s^2), is determined. The results are shown in Fig. 13.

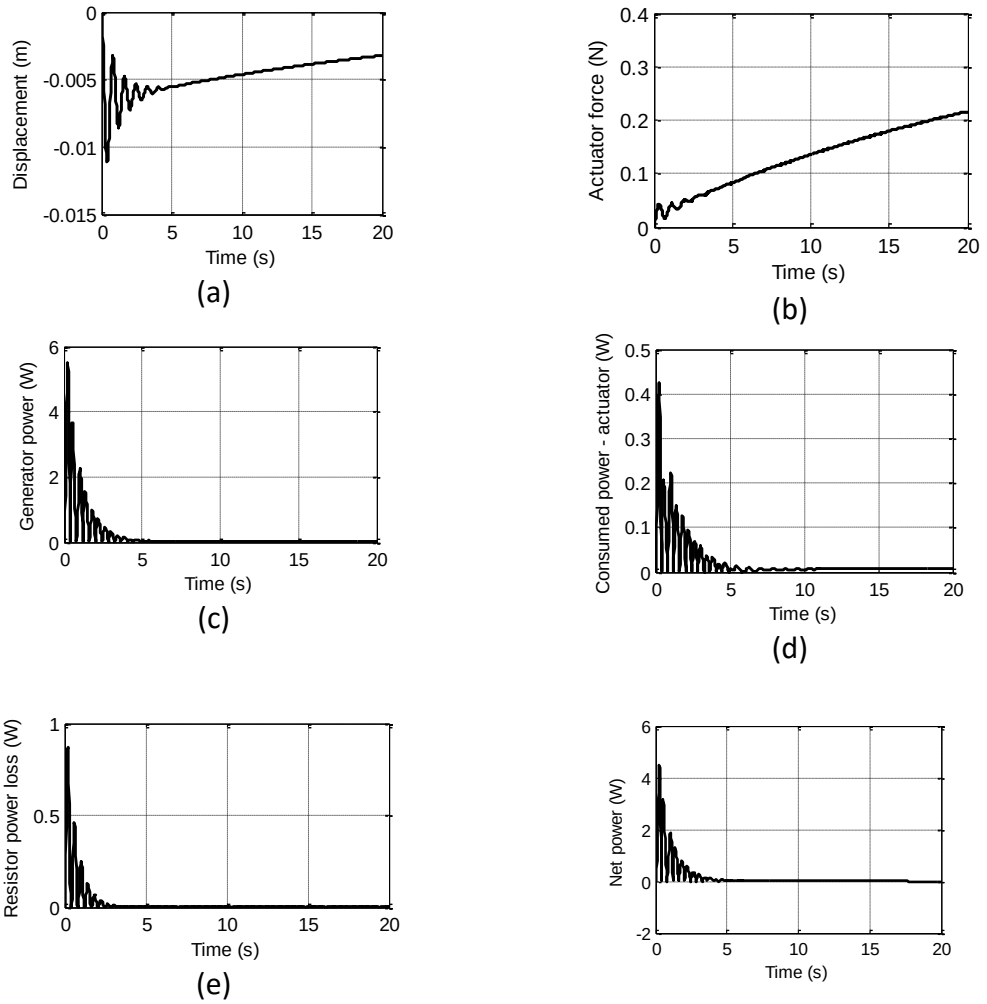

(f)

Fig. 13 (a) Relative displacement, (b) Actuator force, (c) Power produced by the generator, (d) Power consumed by the actuator, (e) Resistor power loss, (f) Available net power.

Further results for the present example are presented in Fig. 14 and Fig. 15. It is seen that self-powered control is feasible with the controller parameter sets 1 and 2 but not with the parameter set 3.

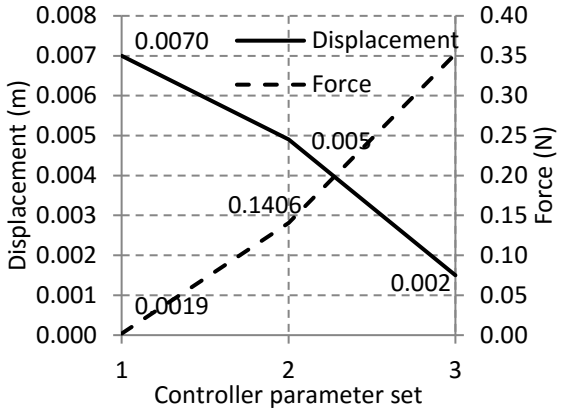

Fig. 14 Displacement of the system with different control parameter sets, and the corresponding control force.

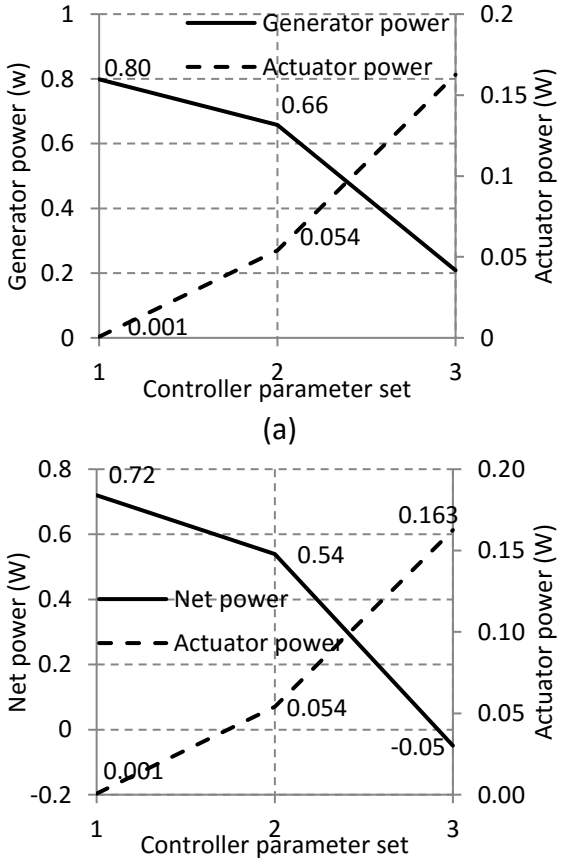

(b)

Fig. 15 (a) Generator power and the consumed actuator power with different controller parameter sets, (b) total available net power with different controller parameter sets.

Now the procedure is repeated with a random excitation of power spectral density (PSD) function as defined by ISO [52]:

$$S_g(\Omega) = C_{sp}\Omega^{-N}$$

where $S_g(\Omega)$ is the PSD function of the input displacement, and Ω is the special frequency. Also, C_{sp} and N are given parameters $N = 2.1$, $C_{sp} = 8.1 \times 10^{-6}$ which provides a noise power of 8.14E-05, for spatial frequency 0.33 cycle/m (this can correspond to a speed of 15 m/s in a vehicle application). The threshold value 0.005m for the relative displacement is used for switching from the generator function to the actuator function in this example.

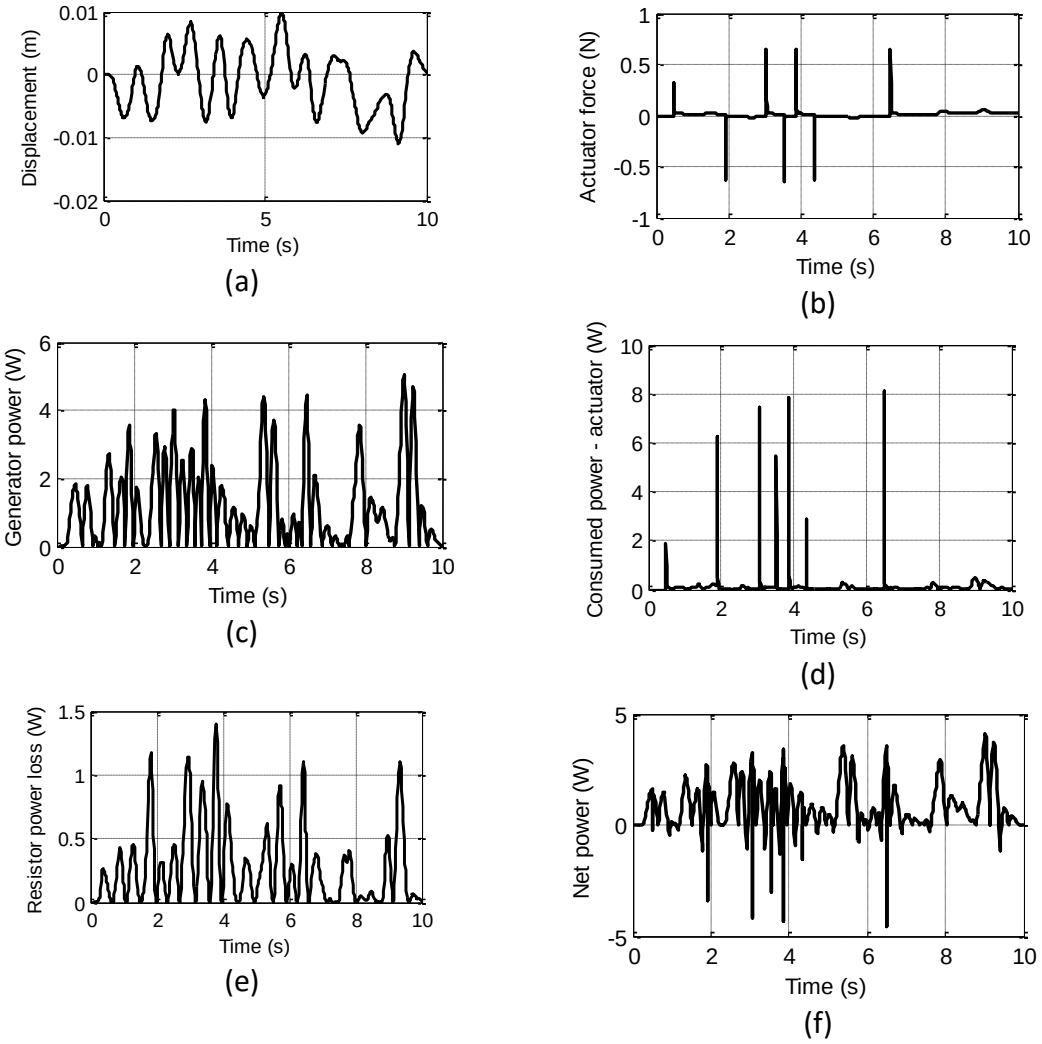

Fig. 16 (a) Relative displacement, (b) Actuator force, (c) Power produced by the generator, (d) Power consumed by the actuator, (e) Resistor power loss, (f) Available net power.

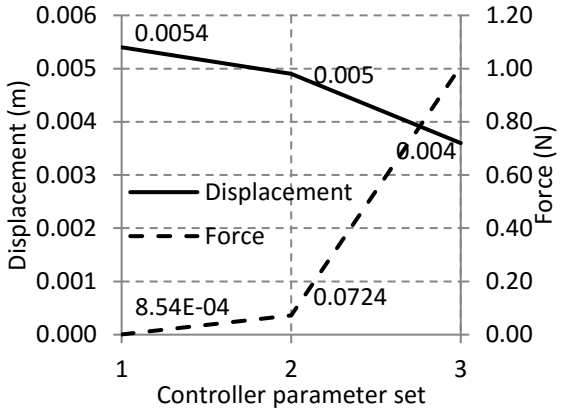

Fig. 17 Displacement of the system for 3 different control parameter sets, and the corresponding control force.

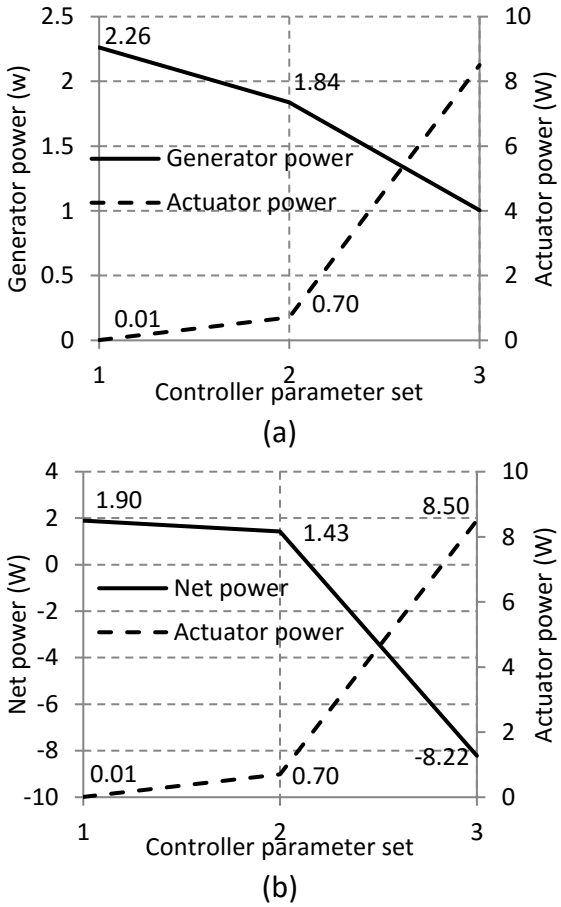

Fig. 18 (a) Generator power and consumed actuator power for different controller parameter sets, (b) Total available net power for different controller parameter sets.

The results in Fig. 18 show that the self-powered control is feasible for controller parameter sets 1 and 2 but not with the parameter set 3. The corresponding response for these controller sets is given in Fig. 17.

The above procedure can be automated for obtaining a suitable control parameters set, which satisfies the performance of the system and the self-powered condition, using OUQ. OUQ can give the tuned PID parameters set (or generalized control parameters) for self-powered condition and achieving acceptable system performance.

Conclusions

Self-powered dynamic systems and the feasibility of developing such systems were discussed in this paper. The regenerative and renewable energy inputs for the energy demand of a system were investigated in terms of a non-dimensional representation of the consumed power. A framework that explores the energy supply and demand while considering uncertainties, constraints, and their optimal bounds was formulated in the context of Optimal Uncertainty Quantification. The feasibility of developing a fully self-powered system was investigated through numerical examples of a regenerative feedback control system. The effect of various control algorithms on the self-powered capability, and obtaining the limits of self-powered systems for specific applications (e.g., fully self-powered vehicles using renewable energy) are investigated in future work [33].

ACKNOWLEDGMENT
The first author wishes to acknowledge Brunel Research and Innovation Fund Award for supporting the research presented in this paper.

NOMENCLATURE

a	a term with power unit correspond to the back-emf voltage
$\mathcal{A}$	an admissible extremal scenario
a_{max}	maximum output acceleration
a_{min}	minimum output acceleration
b	a term with power unit correspond to the PV current
b_m	viscous friction coefficient
c	damping
c_{eq}	equivalent damping
C_{sp}	constant value defined of the PSD
$[c]$	damping matrix
d	sample data
e	Back-electromotive force (back-emf) voltage
f_{max}	maximum external force
F_{max}	maximum actuation force

F_m	motor/actuator force
$f(t)$	external force
$\{f_{act.}\}$	actuation force vector
$\{f_{ext.}\}$	external forces vector
$\{f_{ren.}\}$	equivalent forces generated due to renewable energy inputs
i	input number
I_0	reverse (dark) saturation current
i_a	armature current
I_b	battery current
I_d	diode current
I_{max}	maximum current of the PV cell
I_{PV}	photovoltaic cell current
I_{SC}	short circuit current
I_{SH}	shunt resistor current
J_m	moment of inertia of the rotor
k	Stiffness
k_B	Boltzmann's constant
k_d	derivative controller term
K_e	electric constant (voltage constant) of the motor
k_i	integral controller term
k_p	proportional controller term
K_t	torque constant of the motor
$[k]$	stiffness matrix
L_a	inductance
$\mathcal{L}$	lower bound
m	mass
$[M]$	mass matrix
n	number of inputs
p_c	possible output function of P_c
P_c	consumed power
$P_{d\gamma}$	non-dimensional power

$P_{d\lambda}$	non-dimensional power
P_g	power generation
P_{max}	output upper bound
P_T	sum of consumed power and power loss
q	electron charge
R_a	resistance
R_B	equivalent electrical load of the battery
R_s	resistance correspond to voltage drop in the electrical contacts
R_{SH}	shunt resistance
S_g	power spectral density (PSD)
T	torque
T_c	junction temperature
$\mathcal{U}$	upper bound
X	deterministic input
$\mathcal{X}$	stochastic input
$\{x\}$	displacement vector
$\{\dot{x}\}$	velocity vector
$\{\ddot{x}\}$	acceleration vector
y	base displacement
$\ddot{y}$	acceleration base excitation
$\ddot{y}_{max}$	maximum input acceleration
z	relative displacement
$\dot{z}$	relative velocity
α	+1 or -1 value depending on dive or regenerative modes
γ	a non-dimensional expression for power
θ	estimation of a function
$\dot{\theta}_m$	shaft's rotational velocity
λ	a non-dimensional expression for power
μ	a non-dimensional force parameter
μ_i	probability measure of the input i
σ	a non-dimensional term correspond to the voltage motor
φ	lead/roller/ball screw, rotary to linear gear ratio, and efficiency

$\Phi(\mu)$	an arbitrary function
Ω	special frequency

REFERENCES

[1] Khoshnoud, F., Zhang, Y., Shimura, R., Shahba, A., Jin, G., Pissanidis, G., Chen, Y. K., and De Silva, C. W., 2015, "Energy regeneration from suspension dynamic modes and self-powered actuation," *IEEE/ASME transaction on Mechatronics*, Volume: 20, Issue: 5, pp. 2513 - 2524.

[2] De Silva, C. W., Khoshnoud, F., Li, M., and Halgamuge, S. K. (editors), 2015, *Mechatronics: Fundamentals and Applications*, Chapter 12-Self-powered and Biologically Inspired Dynamic Systems, Taylor & Francis / CRC Press, Boca Raton, Florida, USA.

[3] Khoshnoud, F., Dell, D. J., Chen, Y. K., Calay, R. K., de Silva, C. W., and Owhadi, H., 2013, "Self-Powered Dynamic Systems," European Conference for Aeronautics and Space Sciences, Munich, Germany, Paper 275.

[4] Khoshnoud, F., Lu, J., Zhang, Y., Folkson, R., and De Silva, C. W., 2014, "Suspension energy regeneration for random excitations and self-powered actuation," *IEEE International Conference on Systems, Man, and Cybernetics*, San Diego, CA, USA, pp. 2549-2554.

[5] Khoshnoud, F., McKerns, M., De Silva, C. W., Esat, I. I., Bonser, R. H.C., Owhadi, H., 2016, "Self-powered and Bio-inspired Dynamic Systems: Research and Education," *ASME International Mechanical Engineering Congress and Exposition*, Phoenix, Arizona, USA.

[6] Khoshnoud, F., and De Silva, C. W., Edited by Vantsevich, V. V., and Blundell, M. V., 2015, "Advanced Autonomous Vehicle Design for Severe Environments, (Chapter 8: Mechatronics issues of vehicle control and self-powered systems)," IOS Press, Fairfax, VA, USA.

[7] Khoshnoud, F., Sundar, D. B., Badi, N. M., Chen, Y. K., Calay, R. K., and de Silva, C. W., 2013, "Energy harvesting from suspension systems using regenerative force actuators," *International Journal of Vehicle Noise and Vibration*, Vol. 9, Nos. 3/4, pp. 294 - 311.

[8] Khoshnoud, F., Owhadi, H., de Silva, C. W., Zhu, W., and Ventura, C. E., 2011, "Energy harvesting from ambient vibration with a nanotube based oscillator for remote vibration monitoring," *Proc. of the Canadian Congress of Applied Mechanics*, Vancouver, BC.

[9] Williams, C. B., and Yates, R. B., 1996, "Analysis of a micro-electric generator for Microsystems," *Sensors and Actuators A*, 52, pp. 8–11.

[10] James, E. P., Tudor, M. J., Beeby, S. P., Harris, N. R., Glynne-Jones, P., Ross, J. N., and White, N. M., 2004, "An investigation of self-powered systems for condition monitoring, applications," *Sensors and Actuators A*, 110, pp. 171–176.

[11] Roundy, S., Wright, P. K., and Rabaey, J., 2003, "A study of low level vibrations as a power source for wireless sensor nodes," *Computer Communications*, 26, pp. 1131–1144.

[12] Stephen, N. G., 2006, "On energy harvesting from ambient vibration," *Journal of Sound and Vibration*, 293, pp. 409–425.

[13] Wang, Z. L., 2012, "Self-Powered Nanosensors and Nanosystems," Advanced Materials, Volume 24, Issue 2, Special Issue: SI, pp. 280-285, DOI: 10.1002/adma.201102958.

[14] Erturk, A., and Inman, D. J., 2011, "Piezoelectric Energy Harvesting," John Wiley & Sons, West Sussex, UK.

[15] Khoshnoud, F., and De Silva, C. W., 2012, "Recent advances in MEMS sensor technology - Mechanical Applications," *IEEE Instrumentation and Measurement*, Volume 15, Issue 2, pp. 14 – 24.

[16] Ibrahim, S. W., Ali, W. G., 2012, "A review on frequency tuning methods for piezoelectric energy harvesting systems," *Journal of renewable and sustainable energy*, Volume 4, Issue 6.

[17] Stanton, S. C., McGehee, C. C., Mann, B. P., 2010, "Nonlinear dynamics for broadband energy harvesting: Investigation of a bistable piezoelectric inertial generator," *Physica D*, 239, pp.640-653.

[18] Kong, N., and Ha, D. S., 2012, "Low-Power Design of a Self-powered Piezoelectric Energy Harvesting System With Maximum Power Point Tracking," *IEEE Transactions on power electronics*, Volume 27, Issue 5, pp. 2298-2308. DOI: 10.1109/TPEL.2011.2172960.

[19] Scruggs, J. T., 2004, "Structural control using regenerative force actuation networks," Ph.D. Thesis, California Institute of Technology, Pasadena, CA, USA.

[20] Scruggs J. T., and R. E. Skelton, 2006, "Regenerative Tensegrity Structures for Energy Harvesting Applications," *45th IEEE Conference on Decision and Control*, San Diego, pp. 2282.

[21] Nakano, K., Suda, Y., and Nakadai, S., 2003, "Self-powered active vibration control using a single electric actuator," *Journal of Sound and Vibration*, 260, pp. 213–35.

[22] Zuo, L., Scully, B., Shestani, J., and Zhou, Y., 2010, "Design and characterization of an electromagnetic energy harvester for vehicle suspensions," *Smart Materials and Structures*, 19, 045003 (10pp).

[23] Zuo, L., and Zhang, P., 2012, "Energy harvesting, ride comfort and road handling of regenerative vehicle suspensions," *ASME Journal of Vibrations and Acoustics*, Vol. 135 / 011002-1.

[24] Karnopp, D., 1992, "Power Requirement for Vehicle Suspension Systems. *Vehicle System Dynamics*," 21(1), pp. 65–71.

[25] Goldner, R., Zerigian, P., and Hull, J., 2001, "A Preliminary Study of Energy Recovery in Vehicles by Using Regenerative Magnetic Shock Absorbers," *SAE* Paper No. 2001-01-2071.

[26] Kawamoto, Y., Suda, Y., Inoue, H., and Kondo, T., 2007, "Modeling of Electromagnetic Damper for Automobile Suspension," *J. Syst. Des. Dyn.*, 1, pp. 524–535.
[27] Faris, W. F., Ihsan, S. I., and Ahmadian, M., 2009, "A comparative ride performance and dynamic analysis of passive and semi-active suspension systems based on different vehicle models," *Int. J. of Vehicle Noise and Vibration*, Vol. 5, No. 1/2, pp. 116 - 140.
[28] Shen, W.-a., Zhu, S., and Xu, Y.-L., 2012, "An experimental study on self-powered vibration control and monitoring system using electromagnetic TMD and wireless sensors," *Sensors and Actuators A-Physical*, Volume 180, pp. 166-176. DOI: 10.1016/j.sna.2012.04.011.
[29] Dumas, A., Madonia, M., Giuliani, I., and Trancossi, M., 2011, "MAAT, Multibody Advanced Airship for Transport," *SAE Aerotech, Congress & Exposition*, Toulouse, October 2011, Issn 0148-7191.
[30] http://cordis.europa.eu/project/rcn/99650_en.html (Accessed March 2017).
[31] Khoshnoud, F., Chen, Y. K., and Calay, R. K., 2013, "On Power and Control Systems of Multibody Advanced Airship for Transport," *International journal of Modelling, Identification and Control*, Vol. 18, No. 4, 2013.
[32] Lamb, R., Shrestha, A., Wasely, K., Zand, Z., Kongolo, E., and Patel, D., 2015, "Brunel Solar Powered Airship," Brunel University London, MEng project, 2015.
[33] Khoshnoud, F., et. al., Solar-powered airships: towards infinite endurance UAVs, in progress.
[34] Wang, H., Luo, T., Fan, Y., Lu, Z., Song, H., and Blain Christen, J., 2015, "A self-powered single-axis maximum power direction tracking system with an on-chip sensor," Solar Energy 112, pp. 100–107.
[35] Peng, X., Li, Q., and Wang, K., 2015, "Dynamic compensation of Vanadium self powered neutron detectors based on Luenberger form filter," Progress in Nuclear Energy 78 (2015) 190-195.
[36] Liang, Q., Zhanga, Z., Yan, X., Gu, Y., Zhao, Y., Zhang, G., Lu, S., Liao, Q., Zhang, Y., 2015, "Functional triboelectric generator as self-powered vibration sensor with contact mode and non-contact mode," Nano Energy, Volume 14, May 2015, Pages 209–216.
[37] Wang, S., Lin, L., Wang, Z. L., 2015, "Triboelectric nanogenerator as self-powered active sensors," Nano Energy, 11, pp. 436–462.
[38] Ewing, T., Babauta, J. T., Atci, E., Tang, N., Orellana, J., Heo, D., and Beyenal, H., 2014, "Self-powered wastewater treatment for the enhanced operation of a facultative lagoon," Journal of Power Sources, 269, pp. 284-292.
[39] Liu, W., Formosa, F., Badel, A., Wu, Y., and Agbossou, A., 2014, "Self-powered nonlinear harvesting circuit with a mechanical switchstructure for a bistable generator with stoppers," Sensors and Actuators A, 216, pp. 106–115.
[40] Hanashi, T., Yamazaki, T., Tanaka, H., Ikebukuro, K., Tsugawa, W., and Sodea, K., 2014, "The development of an autonomous self-powered bio-sensing actuator," Sensors and Actuators B, 196, pp. 429–433.
[41] Pinyou, P., Conzuelo, F., Sliozberg, K., Vivekananthan, J., Contin, A., Pöller, S., Plumeré, N., and Schuhmann, W., 2015, "Coupling of an enzymatic biofuel cell to an

electrochemical cell for self-powered glucose sensing with optical readout," Bioelectrochemistry, Volume 106, Part A, pp. 22–27.
[42] Li, Y., Cheng, G., Lin, Z.-H., Yang, J., Lin, L., and Wang, Z. L., 2015, "Single-electrode-based rotationary triboelectric nanogenerator and its applications as self-powered contact area and eccentric angle sensors," Nano Energy, 11, pp. 323–332.
[43] Zhu, H. R., Tang, W., Gao, C. Z., Han, Y., Li, T., Cao, X., and Wang, Z. L., 2015, "Self-powered metal surface anti-corrosion protection using energy harvested from rain drops and wind," Nano Energy, Volume 14, pp. 193–200.
[44] Chen, S., Gao, C., Tang, W., Zhu, H., Han, Y., Jiang, Q., Li, T., Cao, X., and Wang, Z. L., 2015, "Self-powered cleaning of air pollution by wind driven triboelectric nanogenerator," Nano Energy, Volume 14, pp. 217–225.
[45] Bai, P., Zhu, G., Jing, Q., Wu, Y., Yang, J., Chen, J., Ma, J., Zhang, G., and Wang, Z. L., 2015, "Transparent and flexible barcode based on sliding electrification for self-powered identification systems," Nano Energy, 12, pp. 278–286.
[46] Meng, X. S., Li, H. Y., Zhu, G., and Wang, Z. L., 2015, "Fully enclosed bearing-structured self-powered rotation sensor based on electrification at rolling interfaces for multi-tasking motion measurement," Nano Energy, 12, pp. 606–611.
[47] Gai, P.-P., Ji, Y.-S., Wang, W.-J., Song, R.-B., Zhu, C., Chen, Y., Zhang, J.-R., and Zhu, J.-J., 2016, "Ultra sensitive self-powered cytosensor," Nano Energy, Volume 19, pp. 541–549.
[48] Jiang, Q., Han, Y., Tang, W., Zhu, H., Gao, C., Chen, S., Willander, M., Cao, X., and Wang, Z. L., 2015, "Self-powered seawater desalination and electrolysis using flowing kinetic energy," Nano Energy, 15, pp. 266–274.
[49] Luo, J., Fan, F. R., Zhou, T., Tang, W., Xue, F., and Wang, Z. L., 2015, "Ultrasensitive self-powered pressure sensing system," Extreme Mechanics Letters 2, pp. 28–36.
[50] Owhadi, H., Scovel, C., Sullivan, T., McKerns M., and Ortiz, M., 2013, "Optimal Uncertainty Quantification," SIAM Review, Vol. 55, No. 2, pp. 271-345.
[51] Owhadi, H., and Scovel, C., 2016, Handbook of Uncertainty Quantification, Springer International Publishing, Switzerland, pp 1-35, DOI 10.1007/978-3-319-11259-6_3-1.
[52] Wong, J. Y., 2001, "Theory of Ground Vehicles (third edition)," John Wiley & Sons, Inc, 2001, New York, NY, USA.

